Title

Cross-strip readouts for photon counting detectors with high spatial and temporal resolution

Journal

IEEE Transactions on Nuclear Science, 51(4)

ISSN

0018-9499

Authors

Tremsin, A S
Siegmund, OHW
Vallerga, J V
et al.

Publication Date

2004-08-01

Peer reviewed

Cross Strip Readouts for Photon Counting Detectors with High Spatial and Temporal Resolution

Anton S. Tremsin, Oswald H. W. Siegmund, John V. Vallerga, Jeff S. Hull, Robert Abiad

Abstract-- **The combination of a photocathode, microchannel plate stack and photon counting, imaging readout, provides a powerful tool for high dynamic range, high spatial resolution, and high timing accuracy detectors for the X-ray to visible light spectral range. Significant improvements in spatial resolution, quantum efficiency and background rate have made these devices attractive for many applications and are being applied to completely new research areas. We describe the latest developments in high resolution cross strip (XS) anode readout for photon counting imaging with microchannel plates (MCP's). We show that the spatial resolution of a MCP detector with the cross strip readout is now limited only by the MCP pore width. For the first time we show images of resolution test masks illustrating the exceptional spatial resolution of the cross strip readout, which at the present time can resolve features on the scale of ~7 μm with MCP gains as low as $6x10^5$. Low gain operation of the detector with high spatial resolution shown in this paper is very beneficial for applications with high local counting rate and long lifetime requirements. The spatial resolution of the XS anode can be increased even further with improved anode uniformity, lower noise front end electronics and new centroiding algorithms. This could be important when MCP's with smaller than existing 6 μm pores become commercially available, thus improving the detector resolution down to the few micrometer scale.**

Index Terms—**Position sensitive detectors, photon counting, high spatial resolution.**

I. Introduction

THE recent advances in photon counting imaging detectors with microchannel plates give a new perspective to their application in state of the art scientific instrumentation. The latest developments in photocathode technology increase the detection efficiency [1] and extend the spectral sensitivity into the near ultraviolet region with the application of group III-V semiconducting materials [2], as well as into visible part of the spectrum where the efficiency of photocathodes is reported to exceed 50% [3]. Emerging new silicon-micromachined microchannel plate technology [4]-[6] opens up a number of new possibilities, such as deposition of new photocathode materials directly onto the surface of MCP's (opaque photocathodes) allowed by the fact that these Si-microchannel plates can withstand high temperatures required during the deposition process. Since the geometrical structure of these MCP's is determined by a lithographical mask the resulting structures are free of fixed pattern distortions and the pore sizes can be reduced down to a micron scale. Advances in microelectronics allow for very high precision timing information for each registered photon/particle, which can be as small as ~100 picoseconds [7], as well as substantial reduction of power consumption - an important factor for astrophysical applications. All of these improvements combined with the high spatial resolution of the cross strip readout, described in this paper, make microchannel plate detectors a very attractive alternative for a number of new imaging applications.

Manuscript received October 29, 2003.

This work was supported by NASA grant #NAG5-11394

The authors are with Experimental Astrophysics Group, Space Sciences Laboratory, University of California, Berkeley, California 94720, USA (telephone: 510-642-4554, e-mail: ast@ssl.berkeley.edu).

II. Detector Hardware

A. Cross Strip Anode Design and Operation

The cross strip anode [8]-[10] is a coarse period (~0.5 mm) multi-layer metal and ceramic cross strip pattern on a ceramic (alumina) substrate. On one surface of the substrate the conductors are fabricated as a set of fingers approximately 0.5mm wide. Then sets of insulating and conducting fingers are applied in the orthogonal direction such that 50% of the bottom layer is left exposed. The top and bottom layers collect the charge from the MCP's with a 50%/50% sharing (Fig. 1.a). The charge cloud is matched to the anode period so that it is collected on several neighboring fingers to ensure that an accurate event centroid can be determined. Each finger of the anode is connected to a low noise charge sensitive amplifier and followed by subsequent analog to digital conversion of individual strip charge values and a software or hardware centroid determination. The center peak of the charge cloud determines the coarse position of the registered photon. The charge cloud centroid can be calculated to a small fraction of the strip period (currently to ~1/100 of the period) by an appropriate software or hardware algorithm, which in the simplest case is just a weighted sum of the strip charges.

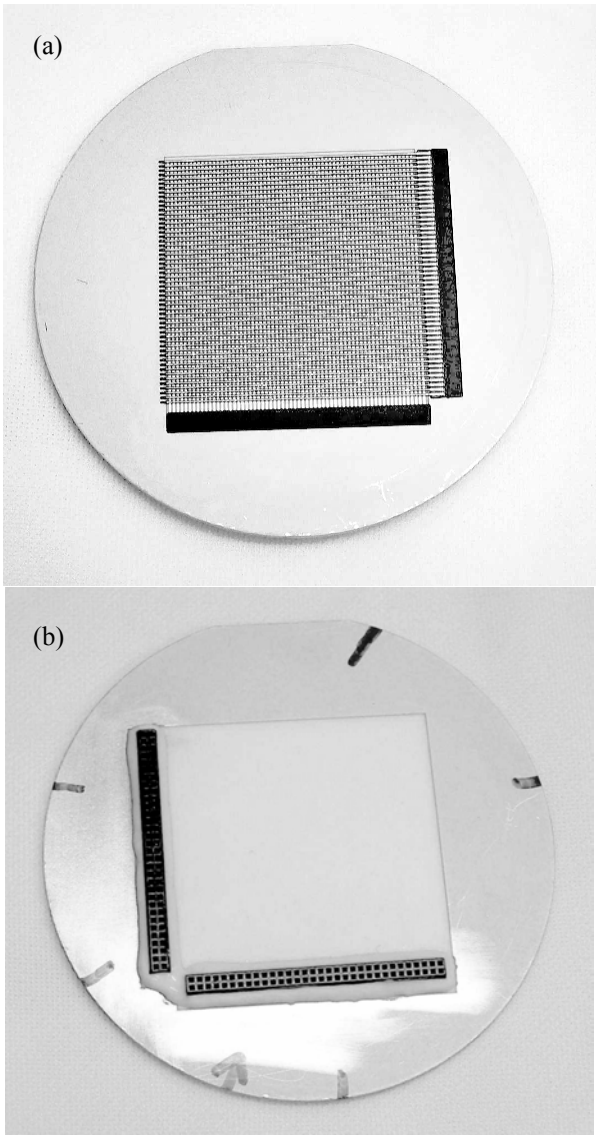

Fig. 1. A photograph of 32x32 mm^2 cross strip anode with 64x56 fingers with period 0.5 and 0.6 mm, respectively. **(a)** front (vacuum) side with sensing finger electrodes; **(b)** back of the anode. The finger electrodes are coupled to the back-end connectors through hermetically sealed vias.

B. Current Implementation of a 32x32 mm^2 Active Area Anode on a Ceramic Substrate

The cross strip anode used in the present study is 32x32 mm^2 with 64x56 fingers on 500 and 600 μm periods for the top and bottom fingers, respectively (Fig. 1.a). Each finger is connected through a hermetically sealed hole to the opposite side of the anode allowing the mounting of all the detector electronics on the outside of the vacuum, and also allowing replacement of the electronics without breaking the vacuum. One of the important features of the existing anode is its compatibility with sealed tube technology requiring particular outgassing and thermal properties of the detector hardware. Thus each finger on the anode is connected to a de-mountable very low noise (~300 electron RMS) preamplifier and shaper, multi-channel, application specific integrated circuit (ASIC) through a back end connector, Fig. 1.b. Mounting preamplifier chips on a custom designed chip carrier board (Fig. 2) allows us to change the ASIC preamplifiers without breaking the vacuum. The peaking time of the ASIC front end chips used in the present setup is about 6 μs. A number of other low noise charge sensitive amplifiers are currently being considered for implementation in our detectors [11], including pixilated readouts developed for high energy physics [12],[13].

Fig. 2. A photograph of back end of the XS anode with the two ASIC chip carrier boards plugged into the back-end connectors.

In the existing configuration the signal from each channel is serially read out from the ASIC with a clock speed of ~5 MHz, postamplified and digitized by the back-end electronics and then transferred into a PC, where the position of the event is determined by a proper centroiding algorithm. The centroiding can also be performed by fast electronics designed by Mead *et. al.* [14], which only takes 5 μs per event. In our existing setup, all finger charge values have to be read out since there is no sparsification (the ability to identify and readout only those fingers with actual signals above a threshold) at the ASIC front end preamplifier. Consequently, the global counting rate of the existing detector is limited by the speed of the ASIC serial readout and did not exceed 10^4 counts per second. We are pursuing several approaches to improve the global readout counting rate capability. Commercial charge sensitive ASIC's that employ sparsification are beginning to become available. Parallel readout ASIC's would also be faster, and we are also pursuing custom designed front ends with sparsification. In the near future we hope to implement new front end ASIC's with sparse readout so that only fingers which collect charge above a controllable threshold are to be digitized for each registered photon.

We did verify that the presence of connectors on the chip carrier and the anode substrate and an extra length of conductor material connecting the pattern fingers to the preamplifiers neither led to any considerable increase of the electronic noise nor introduced any parasitic finger-to-finger coupling. The MCP stack was positioned only 2.2 mm above the anode allowing the possibility to build very compact detectors (Fig. 3). The rear field was controlled by a selection

of an appropriate bias resistor. Our previous thorough studies on the charge footprint in the plane of the anode [15], [16] were very useful for achieving the optimal charge distribution leading to the ultimate best spatial resolution of the detector.

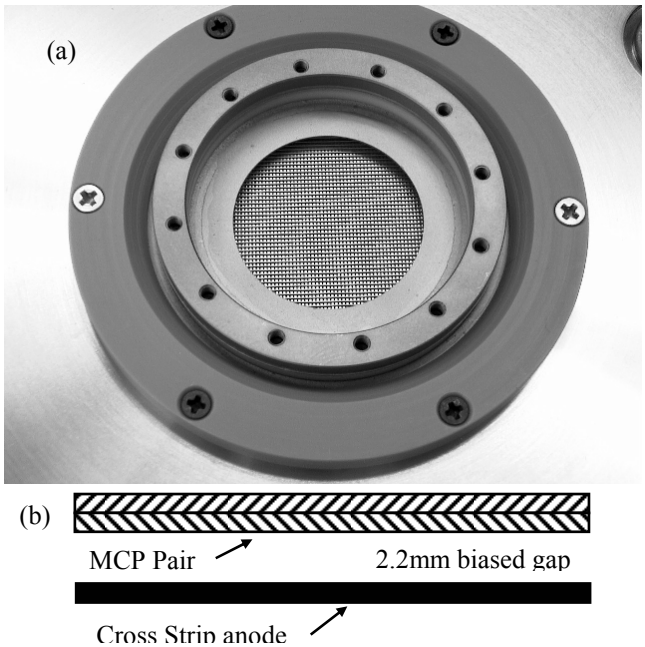

Fig. 3. A photograph of the front (vacuum) side **(a)** and a schematic side view of the detector **(b)** positioned 2.2 mm above the XS anode. The MCP are not installed, permitting the view of the Cross Strip anode input side.

The microchannel plate stack used in the present experiments consisted of a pair of 33 mm diameter, 80:1 L/D, 13 degree biased microchannel plates with 6 μm pores on ~7.2 μm centers with resistance of about 130 MΩ each, stacked in a chevron configuration. All measurements were performed in a vacuum of ~10^{-6} Torr with illumination provided by a mercury vapor penray lamp.

III. Experimental Data

A. Image Linearity

The uniformity of the detector response was studied first with a full field illumination from a penray lamp. We did not try to obtain the most uniform illumination and neither did we select the best microchannel plate stack for these experiments. The reason for the latter was that we wanted to test the performance of the XS anode itself, rather than the quality of the MCP stack. The presence of some small-scale features in the full field illumination image (e.g. dead spots) and their sharpness adds some information on the spatial resolution to the full field illumination image, shown in Fig. 4. That image was obtained with the modified center of gravity centroiding, which took into account all fingers above a threshold fixed at 2% of total per-axis charge. The charge footprint at the plane of the anode was optimized by a proper selection of the rear field and distance in order to achieve the highest image linearity and spatial resolution. The features seen in the image of Fig. 4 correspond to MCP multifiber modulation and some MCP localized defects such as dead pores. No fixed pattern related to the finger period was observed with this optimal charge footprint. The gain of the MCP stack in these measurements was 6x10^5, which is a factor of ~20 less than the gain required for other high resolution photon counting readout techniques.

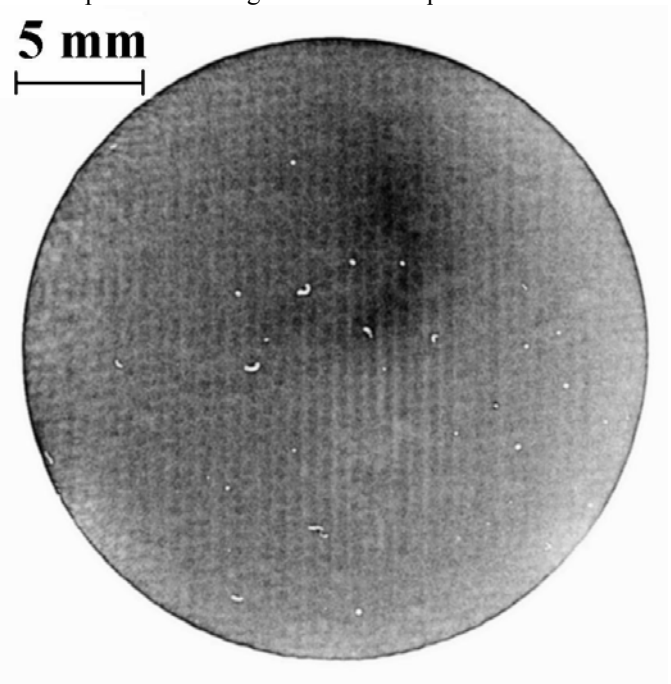

Fig. 4. Full field illumination image obtained at the MCP gain of 6x10^5. Some MCP multifiber modulations and "dead" areas are seen in the image. The dark spot in the middle of the image is due to not completely uniform illumination from a penray lamp.

B. Spatial Resolution

The spatial resolution of our XS readout was investigated with the help of an image mask positioned in direct contact with the input surface of the MCP stack, operating at the same low gain and with the same charge footprint as in the experiments described in the previous section. The image mask used in the measurements contained a set of nine standard US Air Force (USAF) resolution targets deposited on a quartz window. The negative optical microscope image of the resolution mask is shown in Fig. 5. The image obtained by our detector under UV illumination through that image mask is shown in Fig. 6.a. The latter two images are almost identical at first glance. There are some small distortions of the UV image seen under careful examination and they are related to the imperfections in the finger pattern of the existing anode. We believe these imperfections can be eliminated in our next generation of anodes. The section of the UV resolution image, corresponding to only one USAF target is shown in Fig. 6.b, and the section of that image corresponding to only groups 4-7 is shown in Fig. 6.c, illustrating the ultimate resolution of the existing cross strip anode. Apparently, our detector cannot resolve the image mask features smaller than pore-to-pore spacing of the microchannel plates (7.2 μm in our case). This translates to 69 line pairs per mm on the image mask, which is in between Group 6 Element 1 (64 line pairs per mm) and Element 2 (71.8 line pairs per mm). The insert in Fig. 6.c shows histograms through the horizontal and vertical lines of group

6 element 1. This image indicates that the detector resolution reached the theoretical limit. Compare the UV image of Fig. 6.c with the optical image of the same area of the resolution mask positioned on top of a 6 μm pore MCP, Fig. 7. It is clear that it is the MCP pore size that is limiting the spatial resolution of the detector. The spatial resolution of the cross strip anode itself can be better than measured detector resolution, limited by the pore size. The individual 6 μm MCP pores can be imaged with the XS readout, as seen in the image of Fig. 8, showing the Group 5 elements 5 and 6. The resolution mask was in different alignment relative to the MCP stack as compared to the images shown in Fig. 6.

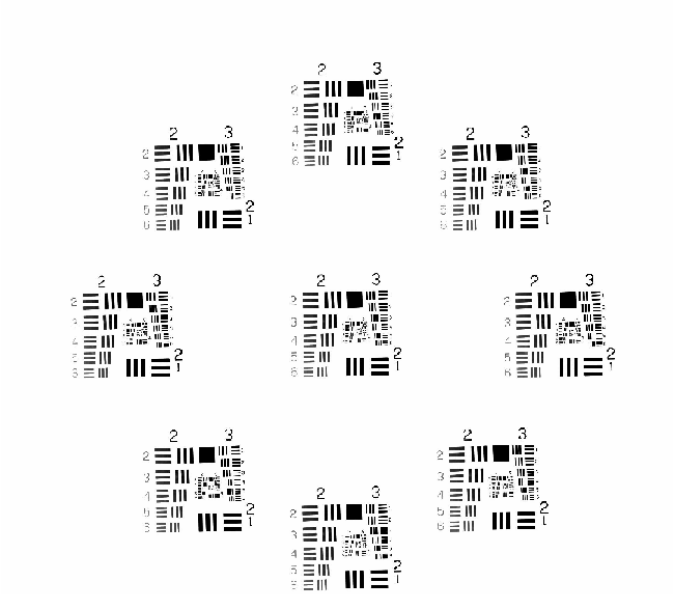

Fig. 5. An optical microscope image (negative) of the resolution mask positioned in direct contact with the input MCP for the characterization of the detector spatial resolution.

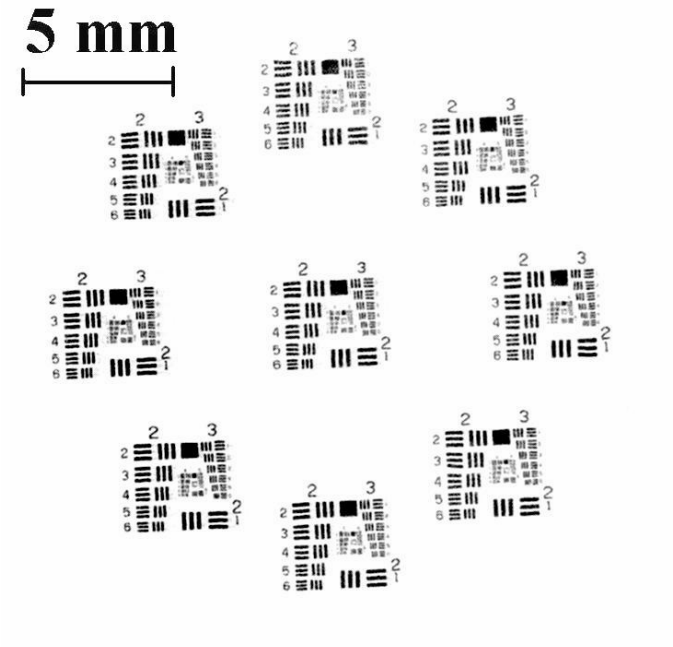

Fig. 6.a. UV image of the resolution mask (shown in Fig.5) obtained with the detector with Cross Strip readout at the detector gain of $6x10^5$.

We want to emphasize that all the images shown in this section are obtained at an MCP gain of ~$6x10^5$, a factor of 20 less than the gain required for high resolution imaging with other methods. The lower gain MCP operation increases local counting rate capability (as a smaller amount of charge needs to be delivered to depleted pores) and also extends the overall lifetime (charge per unit area limits) of MCP operation.

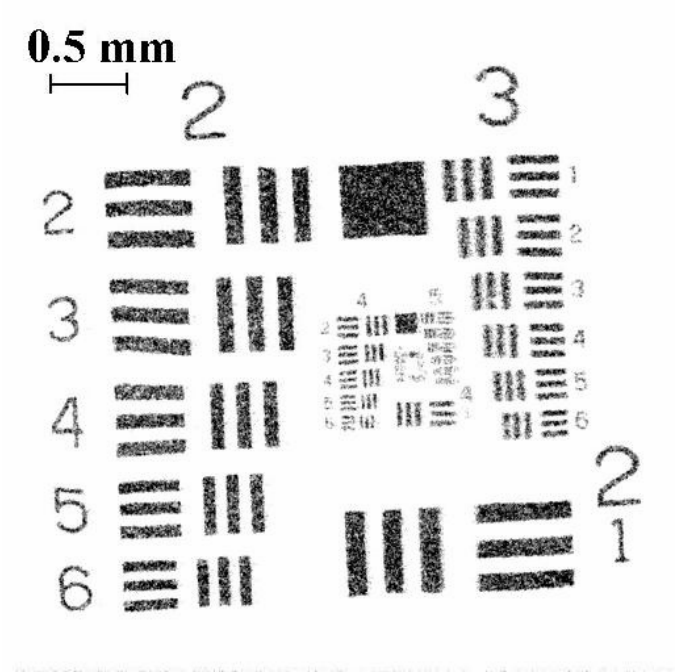

Fig. 6.b. A zoomed section of the UV image shown in Fig. 6.a, containing only one USAF test target with groups from 2 to 7.

We also tried different centroiding algorithms (such as non-linear Gaussian fit, polynomial fit, etc.) in order to achieve the highest spatial resolution and found that the accuracy of simple centroiding is sufficient for current MCP pore dimensions (~6-10 μm) [10].

The noise in the charge-sensing amplifiers is the most important factor determining the accuracy of the cross strip anode position encoding. Since the strip capacitances of 32x32 mm^2 anodes are as small as a few pF, the preamplifier noise was as small as ~500 e RMS and can be reduced to ~350 e for the new generation of front end ASIC's which we are planning to test in the near future. It was the low noise of the preamplifiers, which allowed us to reduce the modal gain of microchannel plate down to $6x10^5$, with spatial resolution still at a few micrometers level.

IV. Acknowledgments

This study was supported by NASA grant #NAG5-11394. Many grateful thanks are extended to our colleague from the Space Sciences Laboratory, Joerg Fisher, for his enthusiastic help with the readout electronics.

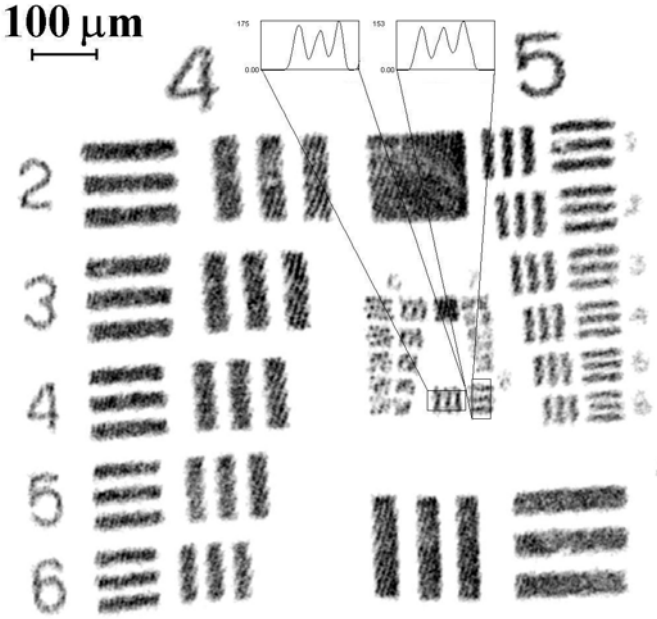

Fig. 6.c. A zoomed central section of the UV image shown in Fig. 6.b, containing only groups 4, 5, 6 and 7. The insert on the image shows histograms through the lines of Group 6 element 1 (64 line pairs per mm) indicating that the spatial resolution of the detector is better than ~7.8 μm. The spatial resolution of the Cross Strip readout itself is even better as some individual 6 μm pores are resolved on that image.

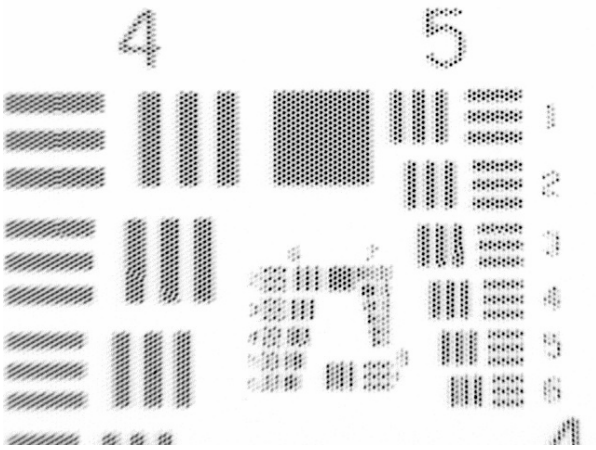

Fig. 7. An optical microscope image (negative) of resolution mask positioned on top of a microchannel plate with 6 μm pores. The image illustrates the ultimate best resolution, which can be achieved with a 6 μm pore MCP. The angular alignment of the pores and the mask determines which elements are still resolved (e.g. group 6 element 2 vertical lines are aligned, while the horizontal lines are not resolved). Compare this optical image with the UV image obtained with the XS detector shown in Fig.6.c.

Fig. 8. Zoomed images of Group 5 elements 5 and 6 of the resolution mask. (left) a negative optical microscope image; (right) UV image obtained with the XS detector.

V. References

[1] A. S. Tremsin, O. H. W. Siegmund, "Quantum efficiency and stability of alkali halide UV photocathodes in the presence of electric field", *Nucl. Instrum. Meth*. vol. A 504, pp.4-8, 2003.

[2] F. S. Shahedipour, M. P. Ulmer, B. W. Wessels, C. L. Joseph, T. Nihashi, "Efficient GaN photocathodes for low-level ultraviolet signal detection ", *IEEE J. Quantum Electrionics*, vol. 38, pp. 333-335, 2002.

[3] Hamamatsu Photonics K.K., http://www.hamamatsu.com

[4] C. P. Beetz, R. W. Boerstler, J. Steinbeck, B. Lemieux, D. R. Winn, " Silicon-micromachined microchannel plates", *Nucl. Instrum. & Meth.* vol. A 442, pp. 443-451, 2000.

[5] A. W. Smith, C. P. Beetz, R. W. Boerstler, D. R. Winn, and J.W. Steinbeck, "Si Microchannel Plates for Image Intensification", *Proc. SPIE*, vol. 4128, pp. 14-22, 2000.

[6] A. S. Tremsin, J. V. Vallerga, O. H. W. Siegmund, C. P. Beetz, R. W. Boerstler, "The latest developments of high gain Si microchannel plates", *Proc. SPIE*, vol. 4854, pp.215-224, 2002.

[7] D. Shapira, T. A. Lewis, L. D. Hulett, "A fast and accurate position-sensitive timing detector based on secondary electron emission", *Nucl. Instrum. & Meth.* vol. A 454, pp. 409-420, 2000; also R. Schletti, P. Wurz, S. Scherer, O. H. W. Siegmund, " Fast microchannel plate detector with an impedance matched anode in suspended substrate technology ", *Rev. Sci. Instr*., vol. 72, pp. 1634-1639, 2001.

[8] O. H. W. Siegmund, A. S. Tremsin, J. V. Vallerga and J. Hull, "Cross strip imaging anodes for microchannel plate detectors", *IEEE Trans. Nucl. Sci.*, vol. 48, pp.430-434, 2001.

[9] O. H. W. Siegmund, A. S. Tremsin, J. V. Vallerga, R. Abiad and J. Hull, "High resolution cross strip anodes for photon counting detectors", *Nucl. Instrum. Methods*, vol.. A504, pp.177-181, 2003.

[10] A. S. Tremsin, J. V. Vallerga, O. H.W. Siegmund, J. S. Hull, "Centroiding algorithms and spatial resolution of photon counting detectors with cross strip anodes", *Proc. SPIE*, vol. 5164, "UV/EUV and Visible Space Instrumentation for Astronomy II", San Diego, August 2003.

[11] T. O. Tumer, V. B. Cajipe, M. Clajus, H. Flores, C. A. Shirley, G. Visser, D. Ward, "Preliminary Test Results of RENA-2 ASIC Developed for Position-Sensitive X-ray and Gamma-Ray Detectors", *IEEE Nuclear Science Symposium*, Norfolk, VA, November 2002.

[12] J.F. Berar, L. Blanquart et al. *"A pixel detector with large dynamic range for high photon counting rates"*, *J. Appl. Crystallography*, vol. 35, pp 471-476, 2002.

[13] X. Llopart, M.Campbell, R. Dinapoli, D. San Segundo, E. Pernigotti, "Medipix2, a 64k pixel readout chip with 55 mm square elements working in single photon counting mode", accepted for publication in *IEEE Trans. Nucl. Sci*.

[14] J. A. Mead, J. A. Harder, N. A. Schaknowski, G. C. Smith, B. Yu, "*Digital Centroid Finding Electronics for Multi-node 2D Detectors*", this conference.

[15] A. S. Tremsin, O. H. W. Siegmund, "Spatial distribution of electron cloud footprints from microchannel plates: measurements and modelling", *Rev. Sci. Instr*. vol 70, pp.3282-3288, 1999.

[16] A. S. Tremsin, O. H. W. Siegmund, "Charge cloud asymmetry in detectors with biased MCPs", *Proc. SPIE*, vol.4497, pp.127-138, 2001.